Topography measurement of scale-model representations of the rough ocean bottom by touch-trigger probe and its implications for spectral characterization

Jason E. Summers, Robert F. Gragg, and Raymond J. Soukup

Acoustics Division, Code 7140
Naval Research Laboratory
Washington, D.C. 20375-5350 USA

Abstract- **Scale models of the ocean bottom exhibiting multiscale roughness having power-law form power-spectral density are useful for validation of deterministic and stochastic rough-surface scattering theories. Such scattering theories require accurate knowledge of the topography of the scale-model surface, which, at acoustic scales, can be measured on a two-dimensional grid using a kinematic-resistive touch-trigger probe and represented by a digital elevation model. Both the discrete representation and the physical measurement process introduce spectral artifacts. While the theoretical relationship describing spectral effects of the discrete representation is well known, this relationship is more complex for the physical measurement process. In the later case, spectral effects result from a combination of random measurement errors and fundamental limitations of probe measurement. Here, a numerical model of the physical measurement process is presented, which is used to simulate spectral effects of probe measurement. While random measurement errors can be controlled for and tend to introduce only an additive white-noise component into the measured power-spectral density, limitations of probe measurement are due to the finite size of the probe stylus and result in a systematic error in the measured power-spectral density for spatial wavenumbers above a critical wavenumber.**

I. INTRODUCTION

Understanding acoustic scattering by rough ocean bottoms requires that theories of rough-surface scattering and their algorithmic implementations be validated by comparison with scattering data from controlled experiments. The scarcity of adequate data on ocean-bottom properties and the consequent inability to conduct systematic studies make validation using scattering data taken from natural sea floors impractical. To circumvent these limitations, small-scale physical models of rough ocean bottoms at sizes manageable for use in an acoustic tank facility can be manufactured. While it is difficult to create physical models that are exact acoustic analogs of real ocean bottoms over a complete set of parameters, a physical model can be constructed to exhibit scattering behavior analogous to a real ocean bottom. In particular, scale models can capture the multiscale roughness

and power-law form power-spectral density (PSD) that characterize some regions of the ocean bottom.

Such validation experiments require that topographies be measured with resolution appropriate to the acoustic frequencies used (100-300 kHz in the studies conducted by the authors) and with accuracy at least commensurate with that to which the other experimental variables are known. At the acoustic scales considered, contact-based techniques, such as touch-trigger probe measurement, operate with sufficient resolution for this purpose. Nonetheless, such techniques can introduce artifacts in both topography measurements, which are required as inputs for deterministic scattering models, and in spectral parameters derived from them, which are required as inputs for stochastic scattering models.

Here, with focus on multiscale rough surfaces having approximately fractal behavior (as illustrated in Fig. 1 and discussed in [1]), the sources of these artifacts are described together with their implications for characterization of surfaces by spectral parameters. Section II describes the discrete representation of topography as digital elevation models (DEMs). In Section III, the physical measurement process is described including mechanical sources of error and a numerical model for simulating measurement of profiles by touch-trigger probe. Spectral consequences of mechanical error are estimated using the numerical model. Finally, fundamental limitations of probe measurement due to the finite size of the probe stylus are described in Section IV. The numerical model is again used to estimate the spectral effects of these errors.

II. DIGITAL ELEVATION MODELS

A. DEM Representation

Acoustic-scattering models typically require as input data either surface topography specified by a DEM, which consists of surface height z measured on a regular x-y grid having sampling intervals Δx and Δy, or, in the case of stochastic theories, parameters derived from PSD estimates $\hat{S}(k)$ made from DEMs.

Report Documentation Page		*Form Approved* *OMB No. 0704-0188*

1. REPORT DATE **01 SEP 2006**	2. REPORT TYPE **N/A**	3. DATES COVERED **-**	
4. TITLE AND SUBTITLE **Topography measurement of scale-model representations of the rough ocean bottom by touchtrigger probe and its implications for spectral characterization**		5a. CONTRACT NUMBER	
		5b. GRANT NUMBER	
		5c. PROGRAM ELEMENT NUMBER	
6. AUTHOR(S)		5d. PROJECT NUMBER	
		5e. TASK NUMBER	
		5f. WORK UNIT NUMBER	
7. PERFORMING ORGANIZATION NAME(S) AND ADDRESS(ES) **Acoustics Division, Code 7140 Naval Research Laboratory Washington, D.C. 20375-**		8. PERFORMING ORGANIZATION REPORT NUMBER	
9. SPONSORING/MONITORING AGENCY NAME(S) AND ADDRESS(ES)		10. SPONSOR/MONITOR'S ACRONYM(S)	
		11. SPONSOR/MONITOR'S REPORT NUMBER(S)	

12. DISTRIBUTION/AVAILABILITY STATEMENT **Approved for public release, distribution unlimited**

13. SUPPLEMENTARY NOTES **See also ADM002006. Proceedings of the MTS/IEEE OCEANS 2006 Boston Conference and Exhibition Held in Boston, Massachusetts on September 15-21, 2006. Federal Government Rights, The original document contains color images.**

14. ABSTRACT

15. SUBJECT TERMS

16. SECURITY CLASSIFICATION OF:			17. LIMITATION OF ABSTRACT **UU**	18. NUMBER OF PAGES **6**	19a. NAME OF RESPONSIBLE PERSON
a. REPORT **unclassified**	b. ABSTRACT **unclassified**	c. THIS PAGE **unclassified**			

Standard Form 298 (Rev. 8-98)
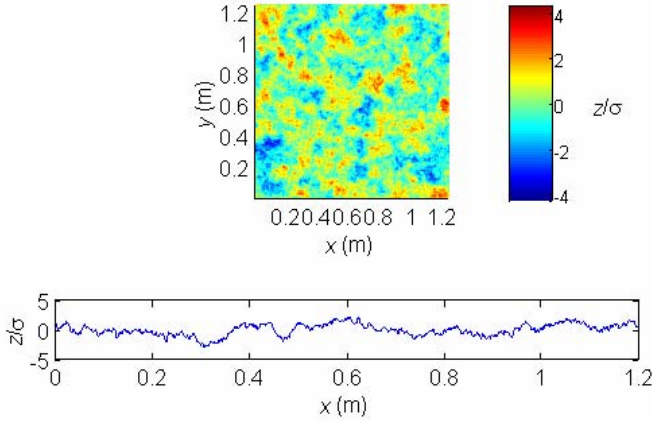Prescribed by ANSI Std Z39-18

Figure 1. Surface topography of a multiscale rough surface having approximately fractal behavior is represented in the color plot by its DEM. The surface shown in the upper figure is an isotropic band-limited fractional Brownian motion surface with spectral strength 3e-5 m^4 and spectral exponent 2.9, as given in (3). The lower figure shows a one-dimensional cut (profile) of the surface. The z axes in both figures have been standardized by dividing by the standard deviation.

B. Spectral Effects

While many scattering theories assume an ideal fractal surface having power-law form PSD for all wave numbers, specifying topography by DEM imposes spectral limitations at large and small spatial wavenumber k due to the finite grid spacing and the finite extent of the model, respectively. The relation between the spatial sampling interval Δx and the maximum resolvable linear spatial wavenumber in each Euclidean dimension is given by the Whittaker-Shannon-Kotel'nikov (WSK) sampling theorem

$$\max\left(|k_x|\right) = \pi / \Delta x . \qquad (1)$$

The relation between the linear extent X of a surface and the minimum resolvable spatial wavenumber in each Euclidean dimension (that for which one wavelength corresponds exactly to the length of the surface) is

$$\min\left(|k_x|\right) = 2\pi / X . \qquad (2)$$

C. Nonspectral Effects

True fractal surfaces are nondifferentiable and therefore have no defined radius of curvature at a particular point. However, the DEM representation of a fractal surface, by band-limiting the PSD, allows for derivatives of the surface to be defined [1].

Likewise, pure power-law PSD is nonintegrable, predicting infinite variance (RMS roughness). The DEM representation, by imposing a small-k cutoff, yields an integrable PSD and predicts a realistic finite variance [1].

D. Choosing a DEM Representation

Though the DEM representation imposes band-limiting on the PSD, all real surfaces have limits to the power-law form of their PSD [1]. Such physical limitations allow for a DEM representation to be chosen that does not alter the PSD. However, if surface parameters are not known *a priori*, the upper spatial frequency of the surface is not known and the sampling interval cannot be chosen to prevent aliasing. In such cases, the sampling interval must be determined through an iterative process [2]. Failure to follow such a process can result in additional errors in the measured topography, which will not be considered further.

In the work of the authors, rough surfaces are band limited for k above those values expected to contribute to scattering, which allows for DEMs to utilize a uniform 1e-3 m grid without aliasing.

III. PHYSICAL MEASUREMENT

A. Touch-Trigger Probe

The kinematic-resistive touch-trigger probe is a robust and accurate means of measuring DEMs to the precision required for acoustic applications. Physically, the touch-trigger probe consists of a small spherical tip of radius ϖ attached to a three-axis microswitch via a slender rod. When measuring the topography of a rough surface, the probe, mounted in a three-axis computer-numerically controlled (CNC) milling machine or coordinate measurement machine (CMM), moves to a sampling location $\mathbf{r}_i = (x_i, y_i)$ and approaches along the z axis (nominally perpendicular to the mean plane of the surface) until contact is made. The recorded height at $\mathbf{r}_i$, reflects a fixed offset from the position of the z-axis carriage of the CNC mill, which is stopped at the time the touch-trigger probe makes contact.

B. Mechanical Sources of Error

The primary requirement of topography measurement is that the recorded height z_i at each point $\mathbf{r}_i$ reflects that of the actual surface at that point. This accuracy is partly determined by mechanical sources of error including (1) positional accuracy of the CNC mill or CMM in the x-y plane, (2) repeatability of the touch-trigger probe, (3) directional asymmetry in the sensitivity of the touch-trigger probe (lobing), and (4) machine-dynamic error (overshoot) due to additional movement of the z-axis carriage after the touch-trigger probe is deflected by the surface. While the effects of these (particularly machine-dynamic error) can be minimized by careful technique [3], they can not be eliminated and are difficult to correct for because they are dependent on the topography of the surface [4, 5].

For the CNC mill used by the authors, positional accuracy is nominally +/- 1.27e-4 m in all axes. Assuming this error to be random, zero mean, and Gaussian distributed, the stated error bounds can be treated as the 95% confidence bounds (+/- 2σ). In a typical CMM, these errors would be far lower and the

errors described below, which effect accuracy in the z-axis only, would dominate.

Repeatability of the touch-trigger probe is determined by both the mechanical behavior of the probe—whether the stylus returns to the same position after each point is sampled—and the electrical behavior of the probe—whether the same amount of deflection is consistently required to trigger the probe. The random error resulting from the failure of the probe to behave identically in all instances is normally distributed with standard deviations on the order of 1e-6 m.

Pretravel is deflection of the stylus prior to triggering. This effect is greatest when the local normal of the probe surface is not parallel to the direction of travel of the probe, which is almost always the case for measurement of rough surfaces. Pretravel also varies with the direction the stylus is displaced, leading to direction dependent pretravel variation, i.e. directional asymmetry. Measurements of pretravel in the literature [4] for a number of touch-trigger probes have found pretravel ranging between 0 and 5.0e-5 m for typical probes. This error depends on a number of factors, including the topography. It is, therefore, difficult to compensate for and is not random but instead correlated to the surface.

Machine-dynamic error depends on the direction of probe motion; for the measurement configuration considered here, it is skewed toward negative z. However, if the overshoot is consistent, its effects can be minimized through calibration. The remaining error due to inconsistency is random and normally distributed.

C. Numerical Simulation

To estimate the spectral effects of mechanical errors, it is necessary to numerically simulate the measurement process. For physical surfaces, true topography can never be exactly known. By numerically simulating the measurement process on numerically generated topography, the effects of measurement can be accurately assessed.

The first step in simulation is the numerical generation of surface topography representing the physical surface. Because the surfaces of interest are isotropic, the simulation can be simplified by considering profiles of surfaces, as shown in Fig. 1. Discrete representations of band-limited fractal profiles have been generated using the method described in [1]. The PSDs of these surfaces follow a power-law form

$$S(k) = \frac{w_2}{(h_0 k)^{\gamma_2}} \quad \text{for } k \in (0, \infty), \quad (3)$$

where h_0 is a reference length, usually taken to be unity, w_2 is the two-dimensional spectral strength in units of $(\text{length})^4$ (i.e.,

the value of the PSD at $k = h_0^{-1}$) and γ_2 is the two-dimensional spectral exponent, except at the extrema of the PSD, as described in [1]. For fractal surfaces, $\gamma_2 \in (2,4]$. Because the surfaces are isotropic, the PSDs of the profiles follow a similar form

$$S_x(k_x) = \frac{w_1}{(h_0 k)^{\gamma_1}} \quad \text{for } k \in (-\infty, \infty). \quad (4)$$

where w_1 is the one-dimensional spectral strength in units of $(\text{length})^4$ (related to w_2 as described in [1]) and $\gamma_1 = \gamma_2 - 1$ is the one-dimensional spectral exponent.

A number of numerical methods have been used in the past to model measurement of profiles [6, 7, 8, 9, 10, 11] and surfaces [12]. These methods model the geometrical interaction of a circular (or spherical) probe tip with an arbitrary profile (or surface) in order to determine the point where the probe first makes contact and, from this, the locus of the probe-tip center. Prior methods of simulation modeled the interaction of the tip only with the sample points of the profile. Here, interaction with the points comprising the profile is modeled as in [8]. Between sample points, linear interpolation is used such that tangent points of the probe tip to line segments between sample points are also considered when determining where the probe first contacts the surface.

As in prior work, deformations of the surface or stylus tip resulting from contact stresses are not considered. However, mechanical errors can be included in this model. As described above, the primary source of mechanical errors in the measurement apparatus used by the authors is positional accuracy of the CNC mill. Such errors can be easily simulated. Errors in the x axis are modeled as described in [13], while errors in the z axis are modeled by choosing $\hat{z}_i$ from a normal distribution centered at the value predicted by the model.

Estimators of PSD for profiles having power-law form PSD must minimize spectral leakage from high-power components at small-k to low-power components at large-k, which biases the estimates [1]. This is accomplished here through windowing and prewhitening the profiles.

D. Spectral Effects

Errors in the z axis resulting from the finite positional accuracy of the CNC mill clearly add a white-noise component to the estimated PSD. Likewise, prior work has shown that errors resulting from the positional accuracy in the x-y plane correspond to additive white noise in the estimated PSD [13].
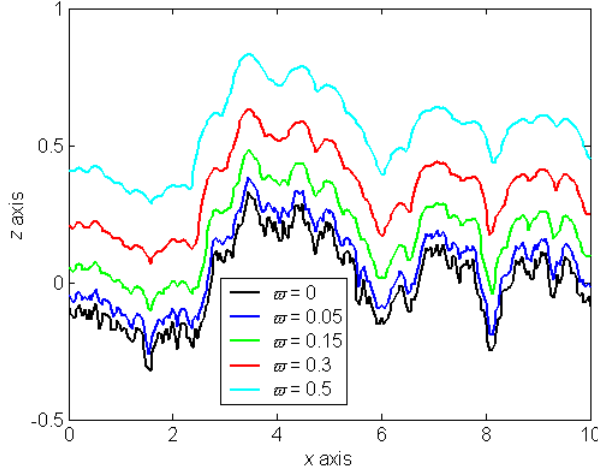
Figure 2. Profile (equivalent to the locus of the probe-tip center for a stylus of radius 0) and loci of the probe-tip center for styli of varying radii, as simulated by the numerical model of measurement described in the text. Axes and probe radii are expressed in arbitrary units.

Figure 3. The locus of the probe-tip center (blue +) and the evolute profile (red -) of a 0.2 radius probe tip are shown for an analytic profile (black -). Axes and probe radii are expressed in arbitrary units.

However, because the positional errors are two orders of magnitude smaller than the sampling interval used and three orders smaller than the typical RMS roughness of a surface being measured (such as that shown in Fig 1), the spectral effects of mechanical errors are negligible in the authors' experimental configuration.

In other conditions, mechanical error can interfere with PSD estimates by biasing the result toward smaller γ, particularly for surfaces having small w and large γ.

IV. EVOLUTE

A. Offset Surfaces

Beyond mechanical limitations of the apparatus itself, contact-based measurements are fundamentally limited in their ability to achieve accuracy by the finite size of the probe tip. Because of this, measurements correspond to the locus of the probe-tip center $\hat{z}_i$ rather than the topography of the surface z_i, as illustrated for various probe radii in Fig. 2. Under optimal conditions, $\hat{z}_i$ corresponds to $\tilde{z}_i$, the z coordinate of the ϖ-evolute surface at $\mathbf{r}_i$. The ϖ-evolute surface [14] is formed by offsetting from the surface $z(\mathbf{r})$ by a distance ϖ along its local normal. Only where the positive radius of curvature $\rho(\mathbf{r})$ (defined in [1]) is greater than ϖ is the evolute surface single valued. Thus, if the tip radius satisfies $\varpi \leq \rho(\mathbf{r})$ in the region being sampled, the probe tip will first contact the surface when the center point of the spherical tip intersects the ϖ-evolute surface. In this case, the probe-center surface corresponds exactly to the evolute, as shown in Fig. 3. In those cases for which $\varpi > \rho(\mathbf{r})$, $\tilde{z}_i$ and z_i are no longer related by the evolute.

Instead, the touch-trigger probe reports truncated depths in those valleys, which correspond to the maximum value of the ϖ-evolute surface at that point, as shown in Fig. 5. However, it is not necessarily apparent that a truncated depth has been reported from direct observation of the measured DEM.

B. Evolute Spectra

Though DEMs measured by touch-trigger probe represent $\hat{z}_i$ rather than z_i, the spectra derived from them correspond to the spectra of true topography at all k up to a critical wavenumber k_c, as illustrated in Figs. 5 and 6. For larger k, the PSD of the profile decays approximately as $k^{-\nu}$ where $\nu \in (4,5)$ for surfaces, that is with a slope consistent with a nonfractal surface.
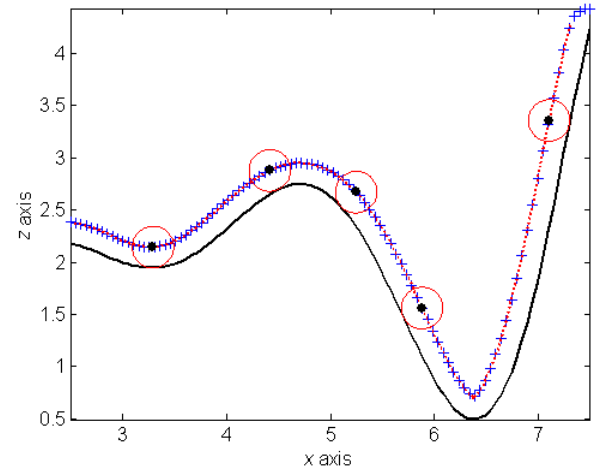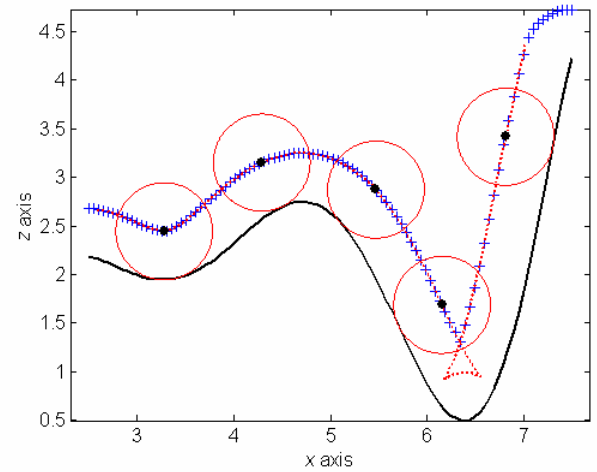

Figure 4. The locus of the probe-tip center (blue +) and the evolute profile (red -) of a 0.5 radius probe tip are shown for an analytic profile (black -). Axes and probe radii are expressed in arbitrary units.

The resulting PSD estimate has a distinct inflection point at $k = k_c$

$$\hat{S}(k) = \begin{cases} S(k) & k \leq k_c \\ S(k_c)\dfrac{k_c^{\nu}}{k^{\nu}} & k \geq k_c \end{cases}. \qquad (5)$$

which serves as a *post hoc* indicator of the scale at which details in the measured DEM are no longer accurate.

Church and Takacs [15] first proposed this behavior, which numerical experiments by Wu confirmed [10]. Later work [11, 12] has shown that, for a given ϖ, k_c is not simply related to the mean curvature of the surface, as conjectured in [15].

Qualitatively, the relationship between probe radius and the measured PSD can be simply explained. Fractal surfaces only have a finite minimum positive radius of curvature if the power-law form of the PSD is truncated at large k. In this way, the value of k at which the PSD is truncated partially determines the minimum positive radius of curvature: larger values of k allowing for smaller minimum positive radii of curvature. If the surface is probed with a stylus having a radius smaller than the minimum radius of curvature, $\hat{z}_i$ corresponds to $\tilde{z}_i$ and $\hat{S}(k)$ is identical to $S(k)$ for all k. However, if the surface is probed with a stylus having a radius larger than the minimum radius of curvature, $\hat{z}_i$ corresponds, in some sense, to $\tilde{z}_i$ with those regions corresponding to the smallest positive radii of curvature excised. In this sense, it is as though the power-law form of the PSD is effectively truncated at a smaller value of k. However, this truncation need not be abrupt, it is sufficient for the power-law exponent to increase to a value corresponding to a nonfractal surface $(\gamma_2 > 4)$, for which radii of curvature are defined.

C. Probe-Radius Compensation

When scattering models require as input the actual surface topography, it must be inferred from the measured DEM representing the ϖ-evolute surface. Various methods exist for solving this inverse problem, which typically require estimation of the local normal vector for all points on the surface [16, 17, 18]. However, errors occurring when $\varpi > \rho(\mathbf{r})$ cannot be compensated for.

V. CONCLUDING REMARKS

Measurement of multiscale rough surfaces by touch –trigger probe yields artifacts in the measured topography that effect PSD estimates. These artifacts can grouped into two classes (1) mechanical errors and (2) fundamental
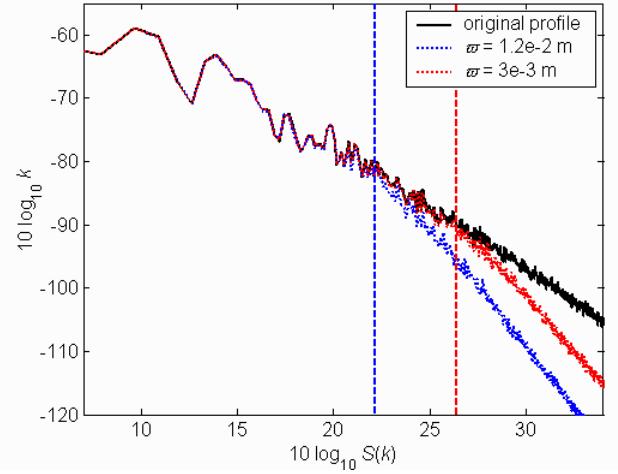
Figure 5. PSD estimates made from the loci of the probe-tip center generated by simulating the measurement of 100 profiles taken from a band-limited fractional Brownian motion surface with spectral strength 3e-5 m^4 and spectral exponent 2.9 are made for two stylus radii and compared with the PSD estimate of the true profiles. Vertical lines indicate the critical wavenumber for the radii. Units are in MKS.

limitations of probe measurement. Which of these classes and which error type within each class dominates depends on both the apparatus used and the surface being measured.

In the spectral domain, mechanical errors tend to introduce additive white noise, which biases the PSD estimates toward smaller spectral estimates and particularly affects surfaces with small spectral strength and large spectral exponents. In contrast, the finite radius of the probe tip biases PSD estimates toward larger spectral exponents above a critical wavenumber k_c. Surfaces having large spectral strength and small spectral exponents are most affected due to their smaller minimum positive radii of curvature.

The effects of errors in PSD estimates can be readily estimated using stochastic scattering models. In the case of deterministic models, however, the effects of measurement artifacts are less obvious. It is unclear, for example, how the scattering predicted from an evolute surface differs from that predicted from the true topography.
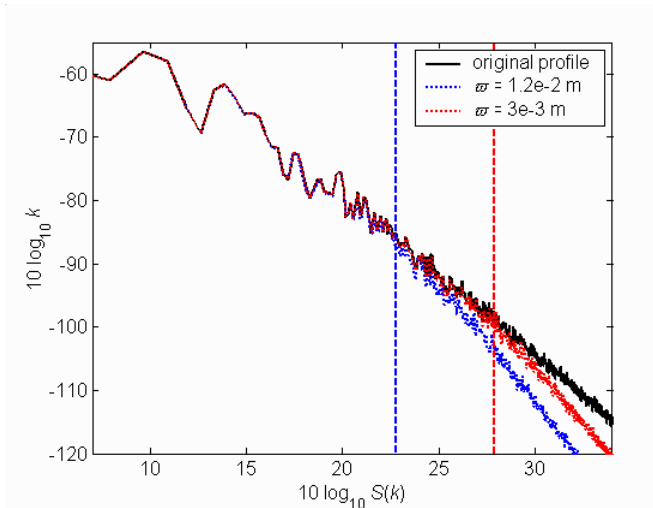
Figure 6. PSD estimates made from the loci of the probe-tip center generated by simulating the measurement of 100 profiles taken from a band-limited fractional Brownian motion surface with spectral strength 4e-4 m^4 and spectral exponent 3.5 are made for two stylus radii and compared with the PSD estimate of the true profiles. Vertical lines indicate the critical wavenumber for the radii. Units are in MKS.

REFERENCES

[1] J.E. Summers, R.J. Soukup, and R.F. Gragg, "Characterization and fabrication of synthetic rough surfaces for acoustical scale-model experiments," U.S. Naval Research Laboratory, Washington, D.C., NRL.MR-MM/7140-05-8871, August 2005.

[2] W.P. Dong, E. Mainsah, and K.J. Stout, "Determination of appropriate sampling conditions for three-dimensional microtopography measurement," *Int. J. Mach. Tools Manufact.*, vol. 36, pp. 1347-1362, 1996.

[3] F.M.M. Chan, E.J. Davis, T.G. King, and K.J. Stout, "Some performance characteristics of multi-axis touch trigger probe," *Meas. Sci. Technol.*, vol. 8, pp. 837-848, 1997.

[4] W. Tyler Ester et al., "Practical aspects of touch-trigger probe error compensation," *Prec. Eng.*, vol. 21, pp. 1-17, July 1997.

[5] C. Dong, C. Zhang, B. Wang, and G. Zhang, "Prediction and compensation of dynamic errors for coordinate measuring machines," *J. Manufact. Sci. Eng.-Trans. ASME*, vol. 124, pp. 509-514, August 2002.

[6] V. Radhakrishnan, "Effect of stylus radius on the roughness values measured with a tracing stylus," *Wear*, vol. 16, pp. 325-335, 1970.

[7] J. I.McCool, "Assessing the effects of stylus tip radius and flight on surface topography measurement," *J. Tribol.-Trans. ASME*, vol. 106, pp. 202-210, 1984.

[8] W.R. DeVries and C.-J. Li, "Algorithms to deconvolve stylus geometry from surface profile measurements," *J. Eng. Indust.*, vol. 107, pp. 167-174, May 1985.

[9] V. Mendeleyev, "Dependence of measuring errors of RMS roughness on stylus tip size for mechanical profilers," *Appl. Opt.*, vol. 36, pp. 9005-9009, 1997.

[10] J.-J. Wu, "Spectral analysis for the effects of stylus tip curvature on measuring rough profiles," *Wear*, vol. 230, pp. 194-200, 1999.

[11] J.-J. Wu, "Spectral analysis for the effects of stylus tip curvature on measuring fractal profiles," *Meas. Sci. Technol.*, vol. 11, pp. 1369-1376, 2000.

[12] J.-J. Wu, "Spectral analysis for the effects of stylus tip curvature on measuring isotropic rough surfaces," *Meas. Sci. Technol.*, vol. 13, pp. 720-730, 2002.

[13] D. Tang, "Fine-scale measurements of sediment roughness and subbottom variability," *IEEE J. Ocean Eng.*, vol. 29, pp. 929-939, October 2004.

[14] E.M. Weisstein, "Evolute," from *MathWorld* [Online] Available: http://mathowrld.wolfram.com/Evolute.html.

[15] E. L. Church and P. Z. Takacs, "Effects of non-vanishing tip size on in mechanical profile measurements," in Optical Testing and Metrology, vol. III, C. P. Grover Ed., Proc. SPIE, vol. 1332, 1991, pp. 504-514.

[16] J.R.R. Mayer, Y.A. Mir, F. Trochu, A. Vafaeesefat, and M. Balazinski, "Touch probe compensation for coordinate measurement using kriging interpolation," *Proc. Instn Mech. Eng., Part B, J. Eng. Manufact.*, vol. 211, pp. 11-18, 1997.

[17] S.-R. Liang and A.C. Lin, "Probe-radius compensation for 3D data points in reverse engineering," *Computers in Indust.*, vol. 48, pp. 241-251, 2002.

[18] Z. Wong and Z. Li, "Probe radius compensation of workpiece localization," *J. Manufact. Sci. Eng.-Trans. ASME*, vol. 125, pp. 509-514, February 2003.